Journal of Earth & Statistics
Journal homepage: http://www.Jes.arakut.ac.ir
Doi: 10.22034/JES.2023.2004232.1033
Ministry of Science, Research & Technology
Arak University of Technology

Analysis of sandy soil liquefaction by reliability method and genetic algorithm

Soheil Torof [1]
[1] Iran, Arak, Arak Islamic Azad University

Article Info

Keywords:
Reliability analysis, probability of liquefaction, reliability index, uncertainty, factor of safety, genetic algorithm.

*Corresponding Author's Email Address:

Abstract

Probability of liquefaction (PL) of sandy soil is based on deterministic analysis to investigate changes in soil resistance and loads caused by dynamic loads such as earthquakes. In addition, there is no possibility to establish a relationship between PL and the factor of safety for the use of these methods. To solve this problem, the statistical analysis and reliability analysis were used. In this article, the reliability analysis was based on the analysis of PL by Seed et al. (1985) and the recommendations of the National Center for Research on Earthquake Engineering (NCEER, 1998). Since the use of this method requires the quantification of uncertainty values in calculations, it is possible to calculate the most probable values related to their uncertainty using statistical moments related to non-deterministic parameters such as mean, variance, standard deviation and probability density function. Then, using the advance first order second moment (AFOSM), the reliability index was calculated by the new method of genetic algorithm and the relationship between PL, the reliability index and the factor of safety was established. For the performance of the proposed method, PL in line 7 of Tehran Metro has been studied based on the results of standard penetration test (SPT) by MATLAB. The results showed the efficiency of the proposed method.

Journal of Earth & Statistics
Journal homepage: http://www.Jes.arakut.ac.ir
Doi: 10.22034/JES.2023.2004232.1033

Nomenclature

SPT	standard penetration test
CPT	Cone Penetration Test
V_s	shear wave velocity
CSR	cyclic stress ratio
CRR	cyclic resistance ratio
τ_{av}	earthquake stress
$a_{\max}$	maximum horizontal acceleration
g	acceleration of gravity
σ_v	total vertical stress
σ'_v	effective vertical stress
r_d	coefficient of reduction of efforts
MSF	magnitude scaling factor
z	depth below ground surface
M_w	magnitude of the earthquake
$(N_1)_{60}$	modified SPT
$(N_1)_{60cs}$	modified SPT According to fine-grained percentage
FC	fine-grained percentage passing through the sieve 200
P_L	Probability of liquefaction
Z	probability function
δ_Z	covariance coefficient
σ_Z	standard deviation
μ_Z	average values of performance function
β	reliability index
$f_z(z)$	probability distribution function
$\Phi(\beta)$	cumulative probability function
X	random variable vector
m	average of the vector values
C	covariance matrix
$G(X)$	operating function
$X_i (i = 1,\ldots,5)$	random variable
ρ	correlation coefficiet

Journal of Earth & Statistics
Journal homepage: http://www.Jes.arakut.ac.ir
Doi: 10.22034/JES.2023.2004232.1033
Ministry of Science, Research & Technology
Arak University of Technology

Introduction

One of the most important phenomena that causes severe damage to buildings and vital flows on young sand alluvium during an earthquake is the phenomenon of liquefaction. If an earthquake-like vibration is imposed on sandy soils, the soil tends to reduce in volume and become compacted. If the soil is unsaturated, this compaction will be possible. But if the soil is saturated and the speed of the movements caused by vibration is so high that the soil cannot be compacted at the same speed and the water in the holes is released through the holes, the water pressure in the holes increases. With the continuation and intensification of the movements, the pore water pressure increases rapidly and with the constant total stress on the soil components, the effective stress or the stress between the particles reduces. There may be situations where the effective stress approaches zero or becomes equal to zero. The occurrence of these conditions causes large changes in the soil and the soil becomes liquefied, such conditions are called liquefaction. This phenomenon appears in the form of significant settlement, creation of openings and cracks, eruption of mud and water, boiling of sand, seepage of water from voids in the ground, and damage to buried pipelines and engineering facilities [1, 2].

One of the methods for evaluating P_L is SPT, which was developed by Seed et al. [3, 4]. In this method, boundary conditions are usually used to separate the liquefied region from the non-liquefied region. These boundary conditions are generally obtained experimentally and conservatively from on-site observations. This experimental method in the development of boundary conditions definitely introduces many uncertainties into the calculations. In addition, most of the evaluation methods are based on deterministic analysis and do not consider the changes in soil resistance and loads caused by earthquakes and are not able to accurately relate to P_L.

A new and comprehensive method to solve the problem is to introduce uncertainties in statistical analysis calculations and especially reliability analysis. Therefore, to quantify uncertainties, statistical moments related to uncertain parameters can be used.

Zhang et al. [5, 6] conducted studies in this field based on seismic cone penetration (CPT) and shear wave velocity (Vs) tests. Also, Hwang et al. [7], using statistical analysis and based on observations of liquefied and non-liquefied areas in the Chi-Chi earthquake, provided a relationship between P_L, cyclic stress ratio and modified SPT.

In the present study, a new method based on reliability and SPT results was presented to evaluate P_L. The proposed method is based on the reliability analysis results of 97 records in line 7 of Tehran Metro.

Methodology

Cyclic stress ratio

One of the quantities used to describe the liquefaction properties of sand under seismic conditions is the cyclic stress ratio. To determine the cyclic stress ratio (CSR), Seed et al. [3, 4] proposed the following equation:

$$CSR = (\tau_{av}/\sigma'_v) = 0.65(a_{\max}/g)(\sigma_v/\sigma'_v)(r_d/MSF) \tag{1}$$

Where a_{max} is the maximum horizontal acceleration, σ_v is total vertical stress, σ'_v is vertical effective stress, r_d is the stress reduction factor due to soil flexibility and MSF is the magnitude scale factor of earthquake. In this study, the equations provided by the International Center for Earthquake Engineering Research (NCEER) for the average values of r_d and MSF are used as follows [8]:

$$r_d = \frac{1.0 - 0.4113z^{0.5} + 0.04052z + 0.001753z^{1.5}}{1.0 - 0.4177z^{0.5} + 0.05729z - 0.006205z^{1.5} + 0.00121z^2} \tag{2}$$

$$MSF = \frac{10^{2.24}}{M_w^{2.56}} \tag{3}$$

Where z is the depth of the soil layers from the earth's surface and M_w is the magnitude of the earthquake.

Cyclic resistance ratio

The cyclic resistance ratio (CRR) of the soil is also determined based on one of the soil resistance characteristics. Seed et al. [4] presented a diagram according to Figure 1 to determine this parameter based on the modified SPT of the soil. This diagram for clean sand is approximated by NCEER as follows [6]:

Journal of Earth & Statistics
Journal homepage: http://www.Jes.arakut.ac.ir
Doi: 10.22034/JES.2023.2004232.1033
Ministry of Science, Research & Technology
Arak University of Technology

$$CRR_{7.5} = \frac{1}{34-(N_1)_{60}} + \frac{(N_1)_{60}}{135} + \frac{50}{[10.(N_1)_{60}+45]^2} - \frac{1}{200} \quad (4)$$

Where $(N_1)_{60}$ is the modified SPT and $CRR_{7.5}$ is CRR for earthquakes with a magnitude of 7.5 on the Richter scale. This equation applies to values $(N_1)_{60} < 30$ and for values $(N_1)_{60} \geq 30$, sandy soils are dense enough and the soil does not liquefy.

To apply the effect of fine-grained percentage on CRR, Equations (5) and (6) have been proposed by NCEER. The equations equate fine-grained sandy soils with clean sand [8].

$$(N_1)_{60cs} = \alpha + \beta(N_1)_{60} \quad (5)$$

Here α and β are the coefficients obtained from the following equations.

$$\alpha = \begin{cases} 0.0 & for \quad FC \leq 5\% \\ \exp[1.76-(190/FC^2)] & for \quad 5\% < FC < 35\% \\ 5.0 & for \quad FC \geq 35\% \end{cases}$$

$$\beta = \begin{cases} 1.0 & for \quad FC \leq 5\% \\ 0.99+(FC^{1.5}/1000)] & for \quad 5\% < FC < 35\% \\ 1.2 & for \quad FC \geq 35\% \end{cases} \quad (6)$$

Where FC is fine-grained percentage passing through the sieve 200.

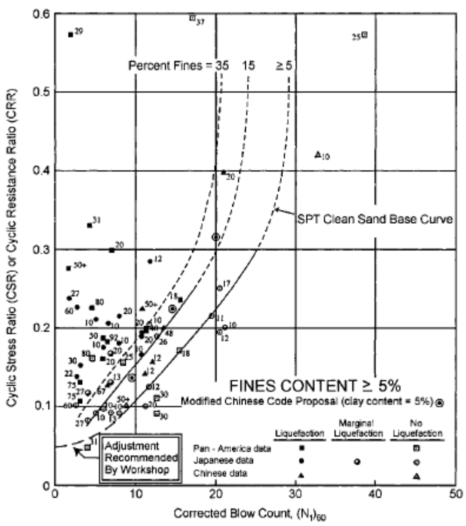

Fig 1. Seed's proposed diagram for determining the periodic CRR based on the modified SPT

Reliability index

The use of the reliability index is suitable to estimate the level of safety against failure by probabilistic analysis methods. In P_L evaluation methods, the performance function can be defined as Z=R-S. If this function is negative, it means failure and occurrence of liquefaction, where S and R represent CSR and CRR, respectively. Since there are some uncertainties in the calculation of S and R, these variables are considered as random variables [7]. If the probability density function and the cumulative probability function Z are expressed by the functions $f_Z(z)$ and $F_Z(z)$, probability of liquefaction (P_L) is equal to the area under the curve in the region $Z = R - S < 0$. Hence:

$$P_L = (Z < 0) = \int_{-\infty}^{0} f_z(z)dz = F_Z(0) \quad (7)$$

Figure 2 shows P_L by the shaded area in the probability distribution function $f_Z(z)$. The reliability index is defined as the inverse of the covariance coefficient (δ_z) and the division of the mean by the standard deviation of the performance function.

$$\beta = \frac{1}{\delta_Z} = \frac{\mu_Z}{\sigma_Z} \quad (8)$$

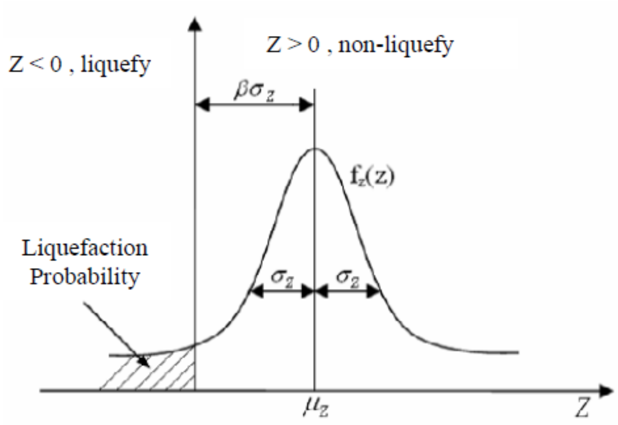

Fig 2. Probability density function related to Z function

If the variables S and R have a normal distribution, according to the principles of probability, the performance function Z=R-S also has a normal distribution $Z \sim (\mu_Z, \sigma_Z^2)$. By substituting the probability density function Z in Equation (7), P_L can be calculated based on Equation (9):

$$P_L = \int_{-\infty}^{0} f_z(z)dz = \int_{-\infty}^{0} \frac{1}{\sqrt{2\pi}\sigma_z} e^{-\frac{1}{2}(\frac{Z-\mu_Z}{\sigma_Z})^2} dz \quad (9)$$

Journal of Earth & Statistics
Journal homepage: http://www.Jes.arakut.ac.ir
Doi: 10.22034/JES.2023.2004232.1033
Ministry of Science, Research & Technology
Arak University of Technology

By substituting $t=(Z-\mu_Z)/\sigma_Z$ in Equation (9), Equation (10) is obtained.

$$P_L=\int_{-\infty}^{-\frac{\mu_Z}{\sigma_Z}}\frac{1}{\sqrt{2\pi}}e^{-\frac{t^2}{2}}dt=\Phi(-\frac{\mu_Z}{\sigma_Z}) \quad (10)$$

$$P_L=\Phi(-\beta)=1-\Phi(\beta) \quad (11)$$

In the equations presented above, P_L is the failure probability, σ_z is standard deviation, μ_z is average values of performance function, β is reliability index and $\Phi(\beta)$ is cumulative probability function. Figure 3 shows changes in P_L to reliability index.

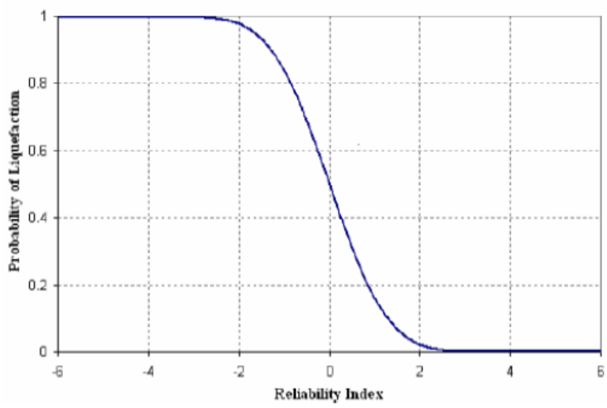

Fig 3. Changes in PL to reliability index.

Genetic algorithm

One of the optimization methods is the new genetic algorithm. The natural basis of the genetic algorithm is based on the competition of living organisms to acquire limited natural resources. The superiority of the winning organisms is due to their individual characteristics, which are largely influenced by their genes. The reproduction of such organisms will cause the multiplication of these genes and as a result worthy offspring. By successively selecting and reproducing the best members, the population will move towards more compromise with the environment, i.e. access to more and better resources. The genetic algorithm calculates the optimal mathematical bound functions by mathematical modeling of the above natural cycle [9, 10].

Several optimization techniques can be used to minimize the reliability index function. Minimization of the reliability index function is one of the constrained optimization problems. One of the optimization methods is the genetic algorithm. Today, these methods have been well developed, although there is still a lot of probability for their development. The genetic algorithm works with a mapping of the set of parameters and not the parameters themselves. This method only needs information about the quality of each solution, while most optimization methods also need the derivatives of the problem, which may not be easy to obtain the derivatives in different problems. While the genetic algorithm does not need the details of the problem. Therefore, it is more flexible than other optimization methods. One of the advantages of this method is that it has an easy mechanism to use the computer, which was done by simulating the problem by MATLAB in the present study. Considering the merits of genetic algorithm in constrained optimization problems, this algorithm has been used in this study.

Results

In geo-technics, load and resistance are often a function of several variables, and it is not possible to calculate the reliability index by direct integration methods, and more advanced techniques must be used. To calculate the reliability index, in this study, AFOSM was used, whose equation is as follows [5, 11].

$$\beta=\min_{X\in F}\sqrt{(X-m)^T C^{-1}(X-m)} \quad (12)$$

Where X is the random variable vector, m is the average of the vector values, and C is the covariance matrix. The minimization should be done on the domain F that belongs to the region of the operating function $(G(X)<0)$. According to the equations presented in the previous section, the variables a_{max}, M_w, σ_v, σ_v' and $(N_1)_{60cs}$ act as random variables. Of course, these parameters have a high correlation that should be included in the calculations. Therefore, by expanding Equation (12), we will have:

$$\beta^2=\min_{G(X)<0}\left\{\left[\frac{(X_1-m_1)^2}{\sigma_1^2}\right]+\left[\frac{(X_2-m_2)^2}{\sigma_2^2}-2\frac{(X_2-m_2)(X_3-m_3)\rho_{23}}{\sigma_2\sigma_3}+\frac{(X_3-m_3)^2}{\sigma_3^2}\right]\left(\frac{1}{1-\rho_{23}^2}\right)+\left[\frac{(X_4-m_4)^2}{\sigma_4^2}-2\frac{(X_4-m_4)(X_5-m_5)\rho_{45}}{\sigma_4\sigma_5}+\frac{(X_5-m_5)^2}{\sigma_5^2}\right]\left(\frac{1}{1-\rho_{45}^2}\right)\right\} \quad (13)$$

Journal of Earth & Statistics
Journal homepage: http://www.Jes.arakut.ac.ir
Doi: 10.22034/JES.2023.2004232.1033
Ministry of Science, Research & Technology
Arak University of Technology

Where X_1 is a random variable of $(N_1)_{60cs}$, X_2 is a random variable of σ_v, X_3 is a random variable of σ'_v, X_4 is a random variable of a_{max}, X_5 is a random variable of M_w, ρ_{23} is the correlation coefficient between X_2 and X_3 variables, ρ_{45} is the correlation coefficient between X_4 and X_5 variables and the performance function. Some numerical techniques can be used to minimize the reliability index function [5]. One of the optimization methods is the genetic algorithm. The natural basis of the genetic algorithm is based on the competition of living organisms for the possession of limited natural resources [12]. One of the advantages of this method is that it has an easy mechanism to use the computer, which was done by simulating the problem by MATLAB in the present study.

Table 1 shows random variables considered in this study in detail. The average values of variables σ_v, σ'_v and $(N_1)_{60cs}$ have been calculated according to 97 records of the study area. Also, the dispersion coefficients of the variables σ_v and σ'_v have been estimated according to the changes in the specific weight of the soil, which generally varies from -1.57 to 2.75 g/cm³ in the study area. Since some variables are correlated, the correlation coefficient between the input variables is shown in Table 2.

Table 1. Random variables

Distribution Function	Dispersion Coefficient	Mean	Random Variable
Normal	0.3	20	$(N_1)_{60cs}$
Normal	0.1	-*	σ_v
Normal	0.15	-*	σ'_v
Normal	0.15	0.36	amax
Normal	0.15	6.3	M_w

*Mean at each depth is calculated

Table 2. R^2 of variables

	$(N_1)_{60cs}$	σ_v	σ'_v	**amax**	M_w
$(N_1)_{60cs}$	1.00	0	0	0	0
σ_v	0	1.00	0.95	0	0
σ'_v	0	0.95	1.00	0	0
amax	0	0	0	1.00	0.9
M_w	0	0	0	0.95	1.00

Discussion

In this study, P_L in line 7 of Tehran Metro has been studied. Tehran is located among important faults that have high seismic power and earthquakes with a magnitude of 6.3 can be predicted [15]. In order to investigate P_L, the information of boreholes drilled in the studied area has been used. The drilling depth in these boreholes ranges from 37 to 56 m and the recorded underground water depth fluctuates between 14 and 17 m. In this study, about 97 records related to 6 boreholes from different parts of the region have been analyzed using programming. For each state, CSR, CRR, reliability index and P_L have been calculated continuously at all depths. The information and studies conducted on boreholes H7-1, H7-2, H7-4, I7-2, I7-3, and I7-4 are presented in Tables 3 to 8, respectively.

Journal of Earth & Statistics
Journal homepage: http://www.Jes.arakut.ac.ir
Doi: 10.22034/JES.2023.2004232.1033

Table 3. Information about borehole H7-1

	Z (m)	σ_v (T/m²)	σ'_v (T/m²)	$(N_1)_{60cs}$	a_{max}	M_w	CRR	CSR	FS	P_L (%)
1	4	6.16	6.16	12	0.36	6.3	0.13	0.001	2.09	32
2	6	9.24	9.24	26	0.36	6.3	0.31	0.001	3.32	44
3	8	12.32	12.32	17	0.36	6.3	0.18	0.001	1.44	44
4	10	15.40	15.40	60	0.36	6.3	0.50	0.002	3.18	44
5	12	18.76	18.76	28	0.36	6.3	0.37	0.002	1.93	44
6	14	24.20	22.20	60	0.36	6.3	0.50	0.002	2.02	43
7	16	29.32	25.32	8	0.36	6.3	0.10	0.003	0.32	43
8	20	39.96	31.96	17	0.36	6.3	0.18	0.004	0.44	44
9	28	61.64	45.64	52	0.36	6.3	0.50	0.006	0.79	42
10	30	67.06	49.06	18	0.36	6.3	0.19	0.007	0.28	43
11	34	77.94	55.94	60	0.36	6.3	0.50	0.008	0.63	43
12	42	99.54	69.54	34	0.36	6.3	0.50	0.010	0.49	37
13	43	102.24	71.24	60	0.36	6.3	0.50	0.010	0.48	31

Table 4. Information about borehole H7-2

	Z (m)	σ_v (T/m²)	σ'_v (T/m²)	$(N_1)_{60cs}$	a_{max}	M_w	CRR	CSR	FS	P_L (%)
1	4	6.32	6.32	17	0.36	6.3	0.18	0.001	3.38	44
2	6	9.48	9.48	23	0.36	6.3	0.26	0.001	3.21	44
3	8	12.64	12.64	62	0.36	6.3	0.50	0.001	4.68	43
4	10	16.04	16.04	49	0.36	6.3	0.50	0.001	3.69	44
5	12	21.44	19.44	52	0.36	6.3	0.50	0.002	2.76	44
6	14	26.80	22.80	51	0.36	6.3	0.50	0.002	2.21	44
7	16	32.16	26.16	45	0.36	6.3	0.50	0.003	1.84	43
8	18	37.52	29.52	36	0.36	6.3	0.50	0.003	1.58	44
9	20	42.94	32.94	42	0.36	6.3	0.50	0.004	1.38	44
10	22	48.36	36.36	44	0.36	6.3	0.50	0.004	1.22	42
11	24	53.78	39.78	38	0.36	6.3	0.50	0.005	1.10	44
12	26	59.24	43.24	39	0.36	6.3	0.50	0.005	1.00	43
13	28	64.70	46.70	60	0.36	6.3	0.50	0.005	0.91	44
14	30	70.16	50.16	60	0.36	6.3	0.50	0.006	0.84	45
15	34	80.92	56.92	60	0.36	6.3	0.50	0.007	0.73	43
16	38	91.52	63.52	15	0.36	6.3	0.16	0.008	0.21	43
17	42	102.16	70.16	32	0.36	6.3	0.50	0.009	0.58	44
18	46	113.12	77.12	60	0.36	6.3	0.50	0.010	0.52	42
19	49	121.34	82.34	60	0.36	6.3	0.50	0.010	0.49	45

Journal of Earth & Statistics
Journal homepage: http://www.Jes.arakut.ac.ir
Doi: 10.22034/JES.2023.2004232.1033

Ministry of Science, Research & Technology
Arak University of Technology

Table 5. Information about borehole H7-4

	Z (m)	σ_v (T/m²)	σ'_v (T/m²)	$(N_1)_{60cs}$	a_{max}	M_w	CRR	CSR	FS	P_L (%)
1	4	6.44	6.44	20	0.36	6.3	0.22	0.001	2.68	43
2	6	9.66	9.66	20	0.36	6.3	0.22	0.001	1.78	29
3	8	12.88	12.88	17	0.36	6.3	0.18	0.002	1.12	21
4	10	16.10	16.10	29	0.36	6.3	0.41	0.002	2.04	43
5	13	20.93	20.93	18	0.36	6.3	0.19	0.003	0.73	38
6	16	28.76	25.76	24	0.36	6.3	0.27	0.004	0.76	42
7	18	33.98	28.98	28	0.36	6.3	0.37	0.004	0.87	42
8	20	39.20	32.20	37	0.36	6.3	0.50	0.005	1.02	37
9	24	49.96	38.96	35	0.36	6.3	0.50	0.006	0.80	26
10	26	55.34	42.34	25	0.36	6.3	0.29	0.007	0.42	43
11	28	60.72	45.72	60	0.36	6.3	0.50	0.008	0.66	39
12	33	74.17	54.17	60	0.36	6.3	0.50	0.009	0.54	43
13	37	85.05	61.05	60	0.36	6.3	0.50	0.011	0.47	43

Table 6. Information about borehole I7-2

	Z (m)	σ_v (T/m²)	σ'_v (T/m²)	$(N_1)_{60cs}$	a_{max}	M_w	CRR	CSR	FS	P_L (%)
1	4	6.52	6.52	12	0.36	6.3	0.13	0.000	2.84	46
2	6	9.78	9.78	10	0.36	6.3	0.11	0.001	1.63	46
3	8	13.04	13.04	13	0.36	6.3	0.14	0.001	1.52	48
4	10	16.30	16.30	25	0.36	6.3	0.29	0.001	2.53	46
5	12	21.56	19.56	33	0.36	6.3	0.50	0.002	3.27	47
6	14	26.82	22.82	20	0.36	6.3	0.22	0.002	1.13	43
7	16	32.08	26.08	32	0.36	6.3	0.50	0.002	2.20	47
8	18	37.66	29.66	12	0.36	6.3	0.13	0.003	0.49	44
9	20	43.24	33.24	16	0.36	6.3	0.17	0.003	0.56	47
10	22	48.82	36.82	44	0.36	6.3	0.50	0.003	1.44	46
11	24	54.40	40.40	60	0.36	6.3	0.50	0.004	1.30	46
12	28	65.20	47.20	60	0.36	6.3	0.50	0.005	1.08	48
13	30	70.60	50.60	60	0.36	6.3	0.50	0.005	1.00	44
14	32	75.94	53.94	24	0.36	6.3	0.27	0.005	0.51	47
15	34	81.28	57.28	19	0.36	6.3	0.20	0.006	0.35	47
16	36	86.62	60.62	18	0.36	6.3	0.19	0.006	0.31	47
17	38	91.96	63.96	20	0.36	6.3	0.22	0.007	0.33	46
18	42	102.56	70.56	19	0.36	6.3	0.20	0.007	0.28	47
19	46	113.16	77.16	17	0.36	6.3	0.18	0.008	0.23	48
20	48	118.46	80.46	11	0.36	6.3	0.12	0.008	0.15	44
21	52	129.06	87.06	11	0.36	6.3	0.12	0.009	0.13	47
22	56	139.66	93.66	13	0.36	6.3	0.14	0.010	0.14	46

Table 7. Information about borehole I7-3

	Z (m)	σ_v (T/m²)	σ'_v (T/m²)	$(N_1)_{60cs}$	a_{max}	M_w	CRR	CSR	FS	P_L (%)
1	4	6.56	6.56	12	0.36	6.3	0.13	0.001	1.69	45
2	6	9.84	9.84	5	0.36	6.3	0.07	0.001	0.62	45
3	8	13.12	13.12	23	0.36	6.3	0.26	0.002	1.66	45
4	10	16.40	16.40	12	0.36	6.3	0.13	0.002	0.68	45
5	12	21.68	19.68	35	0.36	6.3	0.50	0.003	1.95	44
6	16	32.24	26.24	15	0.36	6.3	0.16	0.004	0.42	42
7	18	37.52	29.52	10	0.36	6.3	0.11	0.004	0.26	45
8	22	48.40	36.40	23	0.36	6.3	0.26	0.006	0.45	42
9	24	53.84	39.84	60	0.36	6.3	0.50	0.006	0.79	39
10	26	59.28	43.28	36	0.36	6.3	0.50	0.007	0.71	45
11	32	75.66	53.66	60	0.36	6.3	0.50	0.009	0.56	45
12	38	92.10	64.10	60	0.36	6.3	0.50	0.011	0.46	42

Table 8. Information about borehole I7-4

	Z (m)	σ_v (T/m²)	σ'_v (T/m²)	$(N_1)_{60cs}$	a_{max}	M_w	CRR	CSR	FS	P_L (%)
1	2	3.26	3.26	14	0.36	6.3	0.15	0.000	4.14	43
2	4	6.52	6.52	15	0.36	6.3	0.16	0.001	2.21	45
3	8	13.04	13.04	11	0.36	6.3	0.12	0.001	0.84	43
4	10	16.30	16.30	9	0.36	6.3	0.10	0.002	0.58	44
5	12	21.56	19.56	12	0.36	6.3	0.13	0.002	0.55	42
6	14	26.82	22.82	15	0.36	6.3	0.16	0.003	0.54	41
7	16	32.08	26.08	9	0.36	6.3	0.10	0.004	0.29	43
8	18	37.34	29.34	29	0.36	6.3	0.41	0.004	0.99	44
9	20	42.60	32.60	60	0.36	6.3	0.50	0.005	1.06	44
10	22	47.98	35.98	34	0.36	6.3	0.50	0.005	0.94	43
11	26	58.74	42.74	34	0.36	6.3	0.50	0.007	0.77	43
12	28	64.12	46.12	5	0.36	6.3	0.07	0.007	0.10	31
13	30	69.50	49.50	60	0.36	6.3	0.50	0.008	0.65	42
14	32	74.98	52.98	7	0.36	6.3	0.09	0.008	0.11	44
15	34	80.46	56.46	60	0.36	6.3	0.50	0.009	0.56	44
16	36	85.94	59.94	60	0.36	6.3	0.50	0.010	0.52	43
17	38	91.42	63.42	60	0.36	6.3	0.50	0.010	0.49	43
18	40	96.90	66.90	60	0.36	6.3	0.50	0.011	0.46	39

The important point in the proposed model according to Table 6 is that the factor of safety in rows 4 and 5 are 2.53 and 3.27, respectively and the corresponding P_L is 46% and 47%. As shown, the larger factor of safety will not necessarily mean more safety and therefore less risk of failure. It is also noticeable that the confidence factor in rows 19 and 20 are 0.23 and 0.15, respectively and the corresponding P_L is 48% and 44%. Inversely, it can be seen that a smaller factor of safety necessarily means less safety. As a result, the risk of failure will not be higher.

Journal of Earth & Statistics
Journal homepage: http://www.Jes.arakut.ac.ir
Doi: 10.22034/JES.2023.2004232.1033
Ministry of Science, Research & Technology
Arak University of Technology

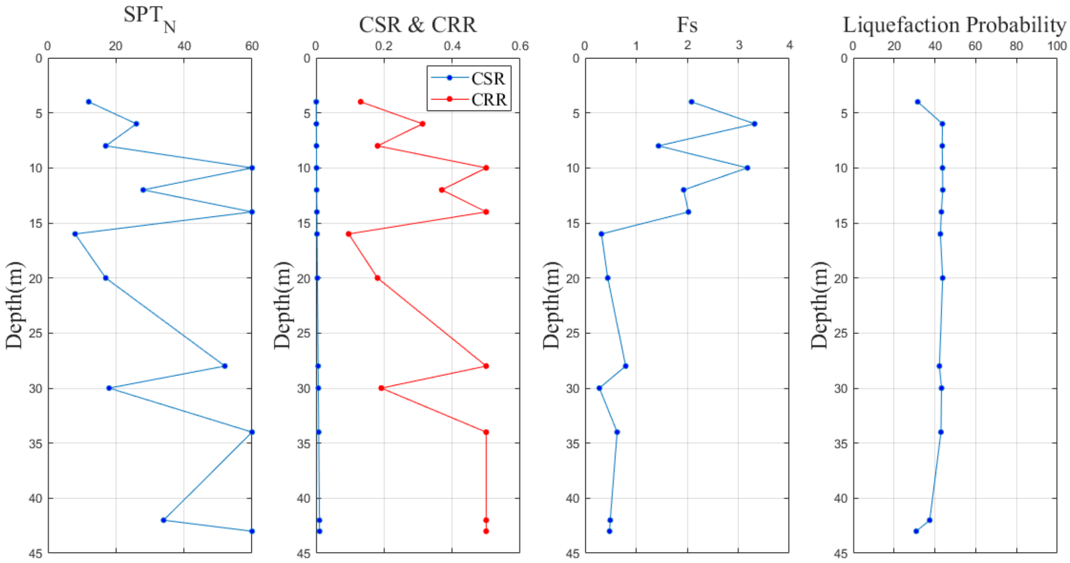

Fig 4. Evaluation of P_L related to borehole H7-1

The curve of changes in P_L obtained from the sample analysis carried out on boreholes as shown in Figures 4 to 9, is a very good guide for engineers to understand the level of risk of liquefaction of soil layers.

As shown in Figure 4, the value of CRR is much higher than that of CSR. By dividing these two parameters together, the factor of safety for liquefaction can be obtained. For this borehole, the factor of safety value is much higher than 1, indicating that liquefaction is unlikely. In the new method mentioned in the report, P_L has been obtained, and this method also shows the probability to be less than 50%.

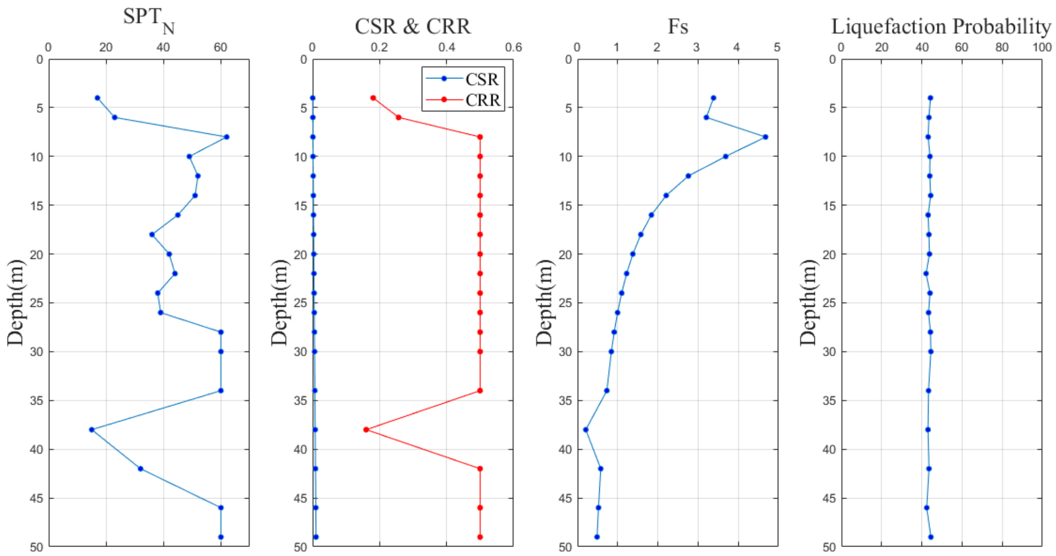

Fig 5. Evaluation of P_L related to borehole H7-2

Journal of Earth & Statistics
Journal homepage: http://www.Jes.arakut.ac.ir
Doi: 10.22034/JES.2023.2004232.1033
Ministry of Science, Research & Technology
Arak University of Technology

As shown in Figures 5 and 6, in boreholes H7-2 and H7-4, SPT_N at different depths is more than 30. Therefore, the value of CRR is accordingly high. In the curve presented, the factor of safety reduces by increasing depth. The reason for this is that SPT_N at surface depths is high and therefore the value of CRR will also be high. On the other hand, the value of CSR increases gradually with depth and its value is low at surface depths. Therefore, the factor of safety value is very high at surface depths.

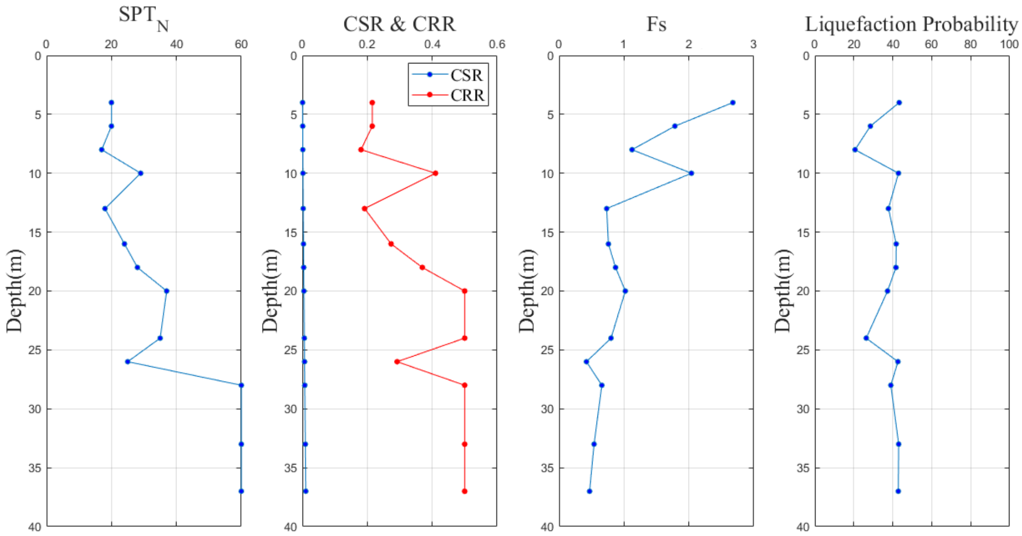

Fig 6. Evaluation of P_L related to borehole H7-4

The factor of safety curve for borehole I7-2 is also obtained for the same reasons as mentioned above (Figure 7). The important point in the SPT and CRR curves is that at the depth where SPT_N is more than 30, the soil resistance has also increased significantly. This article can be used to measure the accuracy of curves.

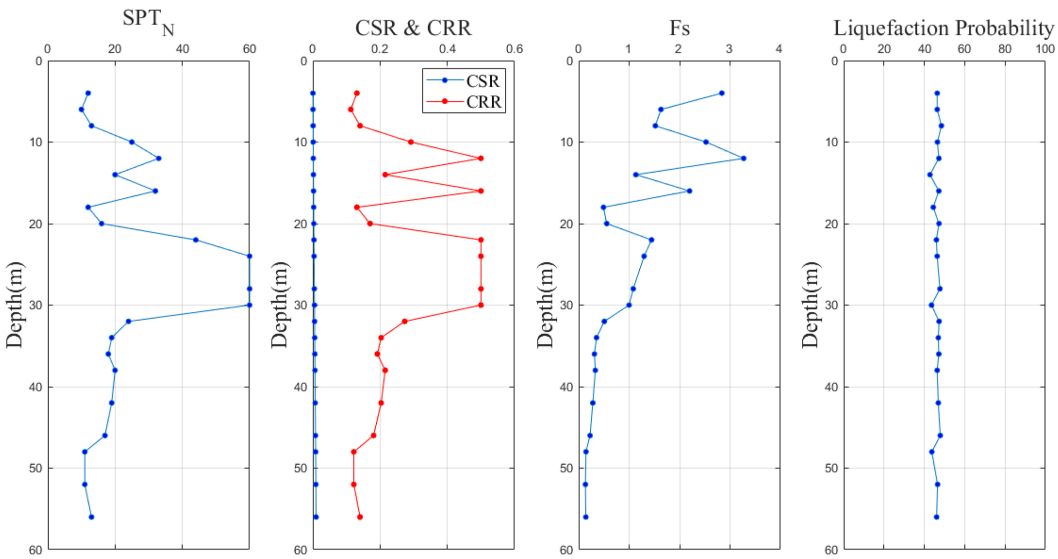

Fig 7. Evaluation of P_L related to borehole I7-2

Journal of Earth & Statistics
Journal homepage: http://www.Jes.arakut.ac.ir
Doi: 10.22034/JES.2023.2004232.1033

Ministry of Science, Research & Technology
Arak University of Technology

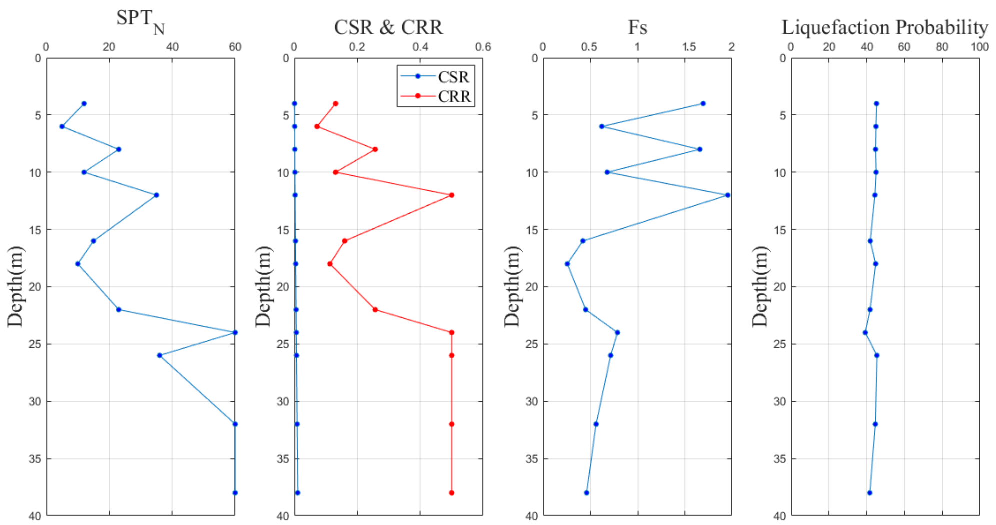

Fig 8. Evaluation of P_L related to borehole I7-3

As shown in Figures 8 and 9, the provided explanations can also be seen in boreholes I7-3 and I7-4. Also, P_L using the proposed new method is consistent with the value of the reliability coefficient obtained from the method of Seed et al.

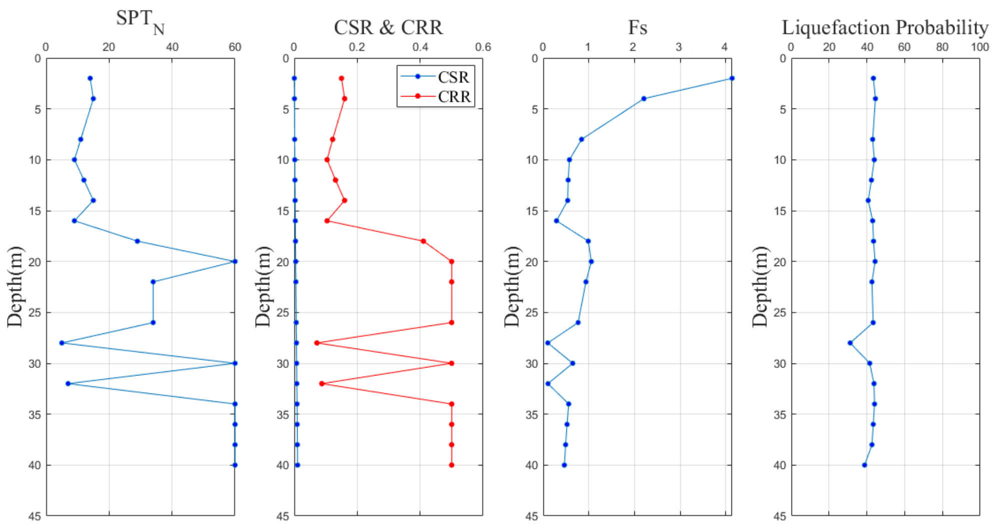

Fig 9. Evaluation of P_L related to borehole I7-4

Journal of Earth & Statistics
Journal homepage: http://www.Jes.arakut.ac.ir
Doi: 10.22034/JES.2023.2004232.1033

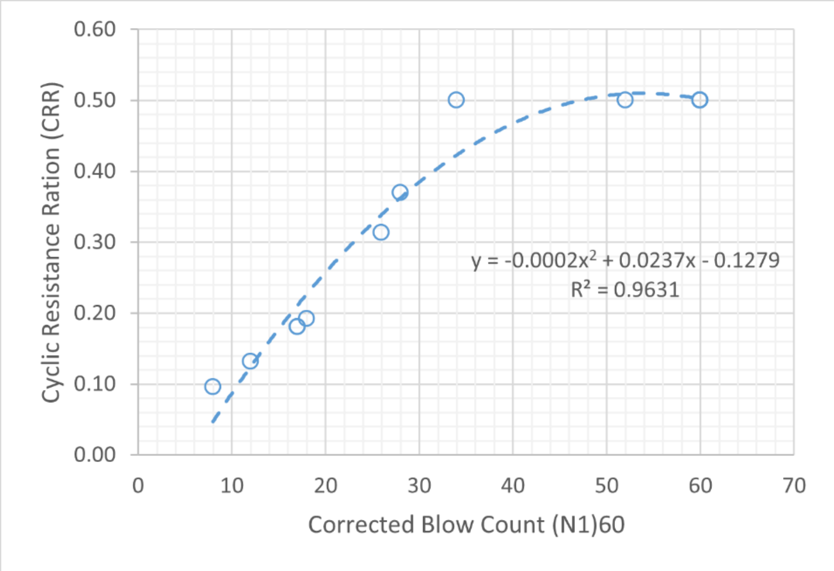

Fig 10. CRR based on the modified Nspt related to borehole H7-1

Using MATLAB program, the proposed model was applied on 97 records in line 7 of Tehran Metro with different variables. Then, using non-linear regression between $(N_1)_{60}$ and CRR by Excel, the relationship between these two variables is shown in Figures 10 to 15. As shown, R^2 has been obtained in the range of 0.94-0.97, indicating good correlation according to the curve presented by Seed et al. [4].

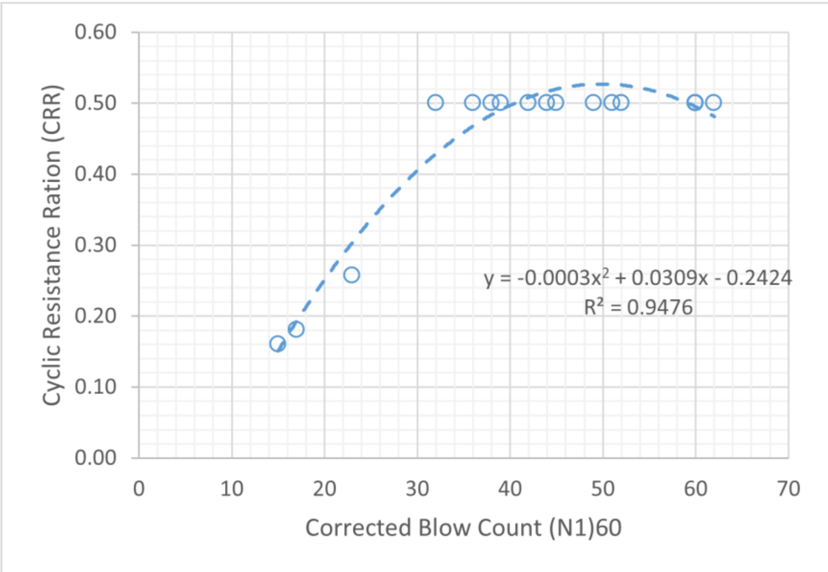

Fig 11. CRR based on the modified Nspt related to borehole H7-2

Journal of Earth & Statistics
Journal homepage: http://www.Jes.arakut.ac.ir
Doi: 10.22034/JES.2023.2004232.1033

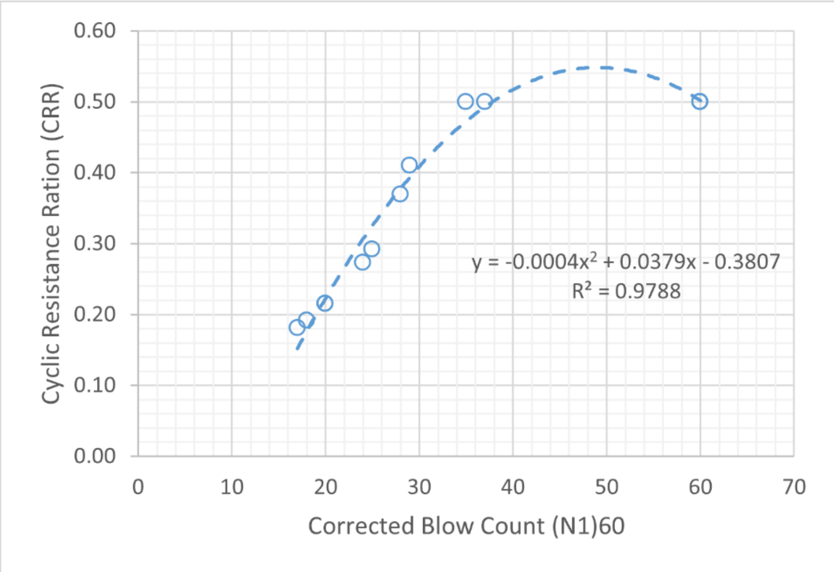

Fig 12. CRR based on the modified Nspt related to borehole H7-4

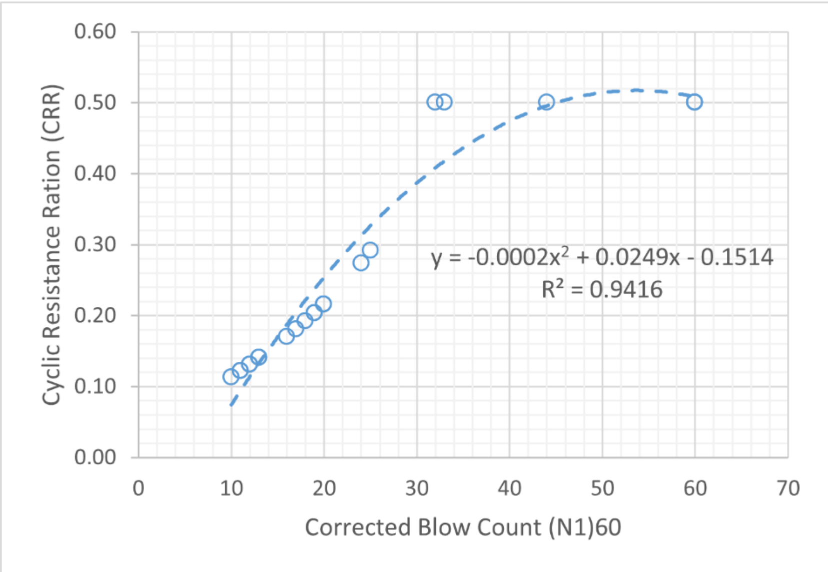

Fig 13. CRR based on the modified Nspt related to borehole I7-2

Journal of Earth & Statistics
Journal homepage: http://www.Jes.arakut.ac.ir
Doi: 10.22034/JES.2023.2004232.1033

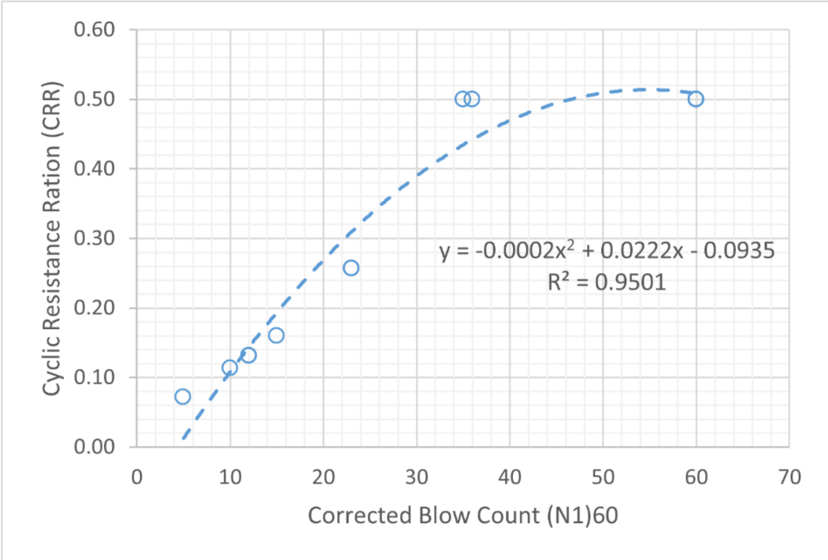

Fig 14. CRR based on the modified Nspt related to borehole I7-3

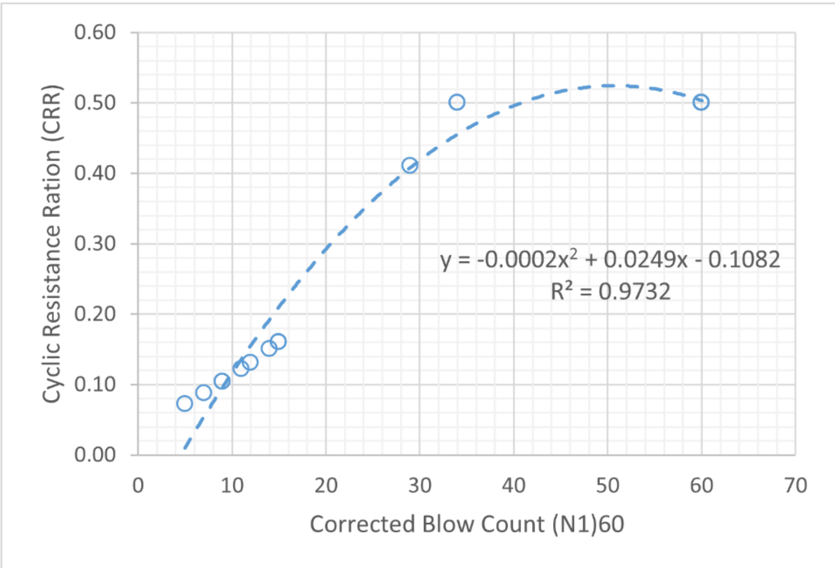

Fig 15. CRR based on the modified Nspt related to borehole I7-4

Conclusion

In this study, a framework was developed to evaluate P_L. According to the results, this method can be used as a practical tool by engineers.

Based on the excavations carried out up to 58 m deep, the subsurface layers include alternating fine-grained and coarse-grained layers. Most of the subsurface layers have been identified as sand layers, whose fine-grained percentage is significant and, in many cases, more than 25%. Sandy and silty layers are mostly observed as thin lenses among sand layers. The thickness of the silty layers is more in the surface depths and especially in one of the boreholes. The plasticity of the layers is very low and they are mostly non-pasty. The thickness of manual soils is 2 m on average.

The range of changes in SPT_N at the project site is very large and it can be seen from lower ones to over 50. According to the results, the soils of the project site are in the range of medium to dense density, while the soil density increases relatively significantly from the depth of 25 m.

Studies have shown that the factor of safety higher than one of the study results of liquefaction does not necessarily mean higher safety and vice versa, but the final judgment should be made along with P_L.

The algorithm designed in this study can be extended to other regions by keeping the generalities and having the required information.

References

1- Marandi S. M., Bagheri Pour M. and Mohammadi Zadeh M. (2002). “Standard penetration field operations and potential control.” 1st Ground Improvement Conference, Amirkabir University of Technology.
2- Mousa Zadeh R., Shoshpasha E. and Mirzagoltabar A. (2006) “Investigating the performance of compression piles in reducing the liquefaction potential of sand beds.” 7th International Congress on Civil Engineering, Tehran.
3- Seed H. B. and Idriss I. M. (1971). “Simplified procedure for evaluating soil liquefaction potential.” J. Soil Mech. Found. Div., Am. Soc. Civ. Eng., 97(9), pp. 1249–1273.
4- Seed H. B., Tokimatsu K., Harder L. F. and Chung R. (1985). “Influence of SPT procedures in soil liquefaction resistance evaluations.” J. Geotech. Eng. Div., Am. Soc. Civ. Eng., 111(12), pp. 1425–1445.
5- Juang C. H., Rosowsky D. V. and Tang W. H. (1999). “Reliability based method for assessing liquefaction potential of soils.” J. Geotech. Geoenviron. Eng., 125-(8), pp. 684–689.
6- Juang C. H., Hui Yang S. and Yuan H. (2005). “Model uncertainty of shear wave velocity-based method for liquefaction potential evaluation.” J. Geotech. Geoenviron.Eng. 131(10), pp. 1274-1281.
7- Hwang J. H., Yang C. W. and Juang D. S. (2004). “A practical reliability-based method for assessing soil liquefaction potential.” J. Soil Dynamics and Earthquake Engineering. 24, pp. 761-770.
8- Youd T. L. and Idriss I. M. (2001). “Liquefaction resistance of soils: summary report from the 1996 NCEER and 1998 NCEER/NSF workshops on evaluation of liquefaction resistance of soils.” J. Geotech. Geoenviron.Eng. 127(10), pp. 817–833.
9- Juang C. H., Chen J. C. and Jiang T. (2001). "Probability framework for liquefaction potential by shear wave velocity." J. Geotech. Geoenviron. Eng. 127(8), pp. 670-678.
10- Low, B. K. and Tang W. H. (1997). "Efficient Reliability Using Spreadsheet." J. Eng. Mech., ASCE, 123(7), pp. 749-752.
11- Baecher G. B. and Chiristian J. T. (2003). “Reliability and statistics in geotechnical engineering.” John Wiley.
12- Goldberg D. E. (1989). “Genetic Algorithms In Search, Optimization, And Machine Learning.”, Addison-Wesley publishing Co.
13- McCully C. and Bleobaum C. L. (1996). “A genetic tool for optimal design sequencing in complex eng. system.”, Structural optimization, Vol. 12, pp. 186-201.
14- Kulhawy F. H. and Tautmann C. H. (1996). “Estimation of in situ test uncertainty.” Uncertainty in the Geologic Environment: From Theory to Practice, GSP No. 58, ASCE, New York, pp. 269–286.
15- Omran Rahvar Consulting Engineers. (2010). Final report of geotechnical and engineering studies for the foundation of 7th line of metro, Tehran.